Soft Matter

Accepted Manuscript

ROYAL SOCIETY OF CHEMISTRY

www.rsc.org/softmatter

From Vesicle to Micelle: Microphase Separation of Amphiphilic Dendrimer Copolymers in a Selective Solvent

Bo Lin*, Lan Liu, Shijie Zhang, Junzuo Huang, Fuan He, Minhua Qi
College of Chemical Engineering, Guangdong University of Petrochemical Technology, Maoming 525000, China
* Corresponding author. Tel: +86-668-2923559. E-mail address: jidalinbo@163.com (B.L).

Abstract: The microphase separation of amphiphilic dendrimer copolymer in a selective solvent with different excluded volume effect (α_S) is investigated by three-dimensional real space self-consistent field theory. The morphological transition of disorder-to-order and order-to-order are observed by systematically regulating the excluded volume effect parameter, interaction parameter of block species, and the spacer length of the second generation of the dendrimer. The ordered segregates of the dendrimer solution are observed with stronger excluded volume effect due to the strong depletion effect of solvent on dendrimer. The relative magnitude between hydrophobic block B and hydrophilic block C is very important for microphase separation, when they are equal ($N_B = N_C$), a structural shift from vesicle to micelle has been found with increasing the interaction parameter, and the region of disordered morphological is controlled by the interfacial free energy (U_{int}); when $N_B > N_C$, the vesicular morphologies overwhelmingly appear in the ordered region and then N_C raises to close to N_B, and the ordered aggregates take a shift from vesicle to micelle. Furthermore, the amphiphilic block C of dendrimer is intended to enlarge to $N_C > N_B$, the micellar morphology is dominant in the ordered regime with stronger excluded volume effect, which contributes to the decrease in the hydrophobic block repulsion that is affected by the decreasing in the entropic free energy ($-TS$). The knowledge obtained from the microphase separation of dendrimer solution induced by the excluded volume effect of selective solvent is full of referential significance in understanding the morphological transition from vesicle to micelle for the amphiphilie in the field of soft matter.

Key words: dendrimer, selective solvent, excluded volume effect, self-consistent field theory.

I. Introduction

Dendrimers are a special class of artificial macromolecules with hyperbranched architecture,[1,2] which leads to unique properties, such as monodispersity, three-dimensional molecules with well-defined size and controllable surface functionalities, good water solubility, and biocompatibility. Accordingly, dendrimers have been found many potential applications in fields of chemical catalysis,[3] stimuli sensitive molecules,[4] drug delivery vehicles[5] and supramolecular chemistry[6]. Amphiphilic dendrimer assemblies are usually preferred relative to their small molecule counterparts, due to their low critical aggregate concentrations (CACs) and high thermodynamic stability. Understanding the structural and phase transition aspects of dendrimers in selective solvent is important and necessary, for applications and functions of dendrimer are tightly linked with their structures.[5] However, the structures of dendrimer are influenced by many factors, such as the generation, spacer length, surface modification, concentration of the additive, and the temperature and pH of the environments.[2] To discover the effect of these factors, various experimental,[7,8] theoretical[2,9] and computational studies[10-12] have been performed recently. For neutral dendrimers, the molecular configurations are usually governed by the quality of the solvent, which reveals the nature of noncovalent interactions between monomers in the dendrimer and solvent molecules.[2,13] In selective solvent, vesicular and micellar type supramolecular assemblies are the most typical morphologies in the self-assembly of dendrimer solution, however, the assemblies of dendrimer are often driven by solvophobic forces and the divergence in whether an amphiphile would form a micelle, a vesicle, or another assembly is determined by the relative position and volume of its functional groups.[13]

Moreover, the selective solvent with different scale in size plays an important role in the morphologies formation of amphiphilie. The effect of solvent molecular size has been widely studied with theoretical and experimental methods in polymer solution.[14] Spontak *et al.*[15] reported that the nanoscale solvent driving the interfacial segregation and central accumulation of the polymer solution. When the solvent

continue to increase in scale with larger molecular weight that is called crowding agent,[14] which can influence the protein folding and aggregation. Generally, the confinement and crowding are two main factors for the properties of bio-molecules, such as, protein folding, self-assembly of amphiphilie. Li *et al.*[16] pointed out the importance of the solvent size and the interaction parameter between the solvent and the hydrophobic monomers in the self-assembly of the polymer solution, meanwhile, an order-to-order transition of morphology from loop-like micelle to line-like micelle then to circle-like micelle was also observed by increasing the solvent molecular size.

As are supplements of the experimental techniques, various theoretical methods have been used to intensively investigate the structures of dendrimers in dilute solutions, including particle-based theory of Brownian dynamics simulation,[2,17,18] molecular dynamics simulation,[19,20] Monte Carlo simulation,[21,22] and field-based methods, such all-atom simulation with Dreiding force field,[23] the static and dynamics method with OPLS force field.[24] Even though the field-based models is independent of the special chemical structure and architecture of dendrimer, it can still reveal the underlying physical significance of the dendrimer systems and compute economically for the particle-based simulations. Field-based simulations on the neutral dendrimers have obtained universal acceptability that the neutral dendrimer has a dense core due to the entropic contributions on the dendrimer systems. As one of field-based method in investigating the motion detail of block copolymer chain, recently, the real-space direct implementation of self-consistent field theory (SCFT) in bulk proposed by Drolet and Fredrickson[25] was extended to deal with the microphase separation behavior of linear or star block copolymers and their blends with different chain length in selective solvent by Wang[2], Tang[26] and Liang[27]. For dendrimers, when the distribution of generations were assumed as concentric shells, de Gennes *et al.*[28] had observed a hollow-core configuration by SCFT modeling a flexible dendrimer with trifunctional monomers and long spacers in athermal solvent, whereas, the results from SCFT without assumption by Boris *et al.*[29] shown that the density profiles decayed from the core through the surface of the dendrimer which seems like a hard-sphere. However, the SCFT is still convenient for understanding the basic

physics controlling the density profiles of the dendrimers. Because the configuration of the dendrimer is balanced by the repulsive of monomer-monomer interaction, say interaction parameters between different block segments (χ_{ij}) used in this work, and the entropic energy penalty for the dendrimer in the configuration of the Gaussian chain model. Here the hollow-core and the hard-sphere configuration are reported as one of the vesicular and the micellar morphology respectively. Their appearances are mainly focused on the motion information of the molecular chain itself in the previous works while ignoring the effect from the external environment of the dendrimer molecule, i.e. the excluded volume effect of the selective solvent (α_S) that adopted in this work.

In this work, a three-dimensional (3D) real space SCFT is used to conduct dendrimer in selective solvent and discuss the disorder-to-order and order-to-order transition especially from vesicle to micelle of the morphologies by regulating the excluded volume effect of selective solvent and the interaction parameters of block species of dendrimer. To archive this objective, we pay particular attention to how the relative magnitude between the hydrophilic block and hydrophobic block effect on the microphase separation of the dendrimer solution.

II. Theoretical Method

In this work, we study a solution system of n_P dendrimer block copolymers with n_S selective solvent molecules. The dendrimer block copolymer (DBC) consists of a flexible hydrophobic core of block A, which is the first generation of the dendrimer, while the second generation of dendrimer including hydrophobic block B and hydrophilic block C. A schematic representation of the architecture of the dendrimer copolymer is shown in Figure 1. Each DBC chain consists of N segments with compositions of f_A, f_B, and f_C for block species of A, B, and C, respectively. We assume the solution system is incompressible with each block segment occupying a fixed volume of ρ_0^{-1} that is equal to the volume of one selective solvent molecule, v_S. Then the total volume of the solution system is $V = n_P N/\rho_0 + n_S v_S$, the volume fraction

of the DBC is $f_P = n_P N / V\rho_0$ and that of the selective solvent is $f_S = 1.0 - f_P$. The ratio of the selective solvent size to block segment is $\rho_S = v_S\rho_0$. In this work, the selective solvent with different molecular size is investigated to take an insight into its effect on the microphase separation of the dendrimer solution. Indeed its influence can be combined together in terms of a single scaling variable, the so-called excluded volume effect parameter $\alpha_S = v_S\rho_0 / N$. Even though the excluded volume parameter amongst the different block segments exists in the dendrimer solution and is defined as the volume occupied by a monomer in a Flory theory of dendrimer that proposed by Boris *et al.*,[29] we have incorporated the excluded volume interaction, and the resulting Gaussian statistics, entirely through coupling to the self-consistent field theory (SCFT) used in this work.

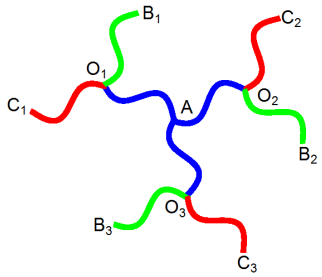

Fig. 1 Schematic representation of the amphiphilic ABC dendrimer block copolymer. Block A (blue) in the first generation and block B (green) in the second generation are hydrophobic, while block C (red) in the second generation is hydrophilic for the selective solvent.

In the SCFT, a mean field ω_i represents the total interaction experienced by a segment i conjugates to the segment density field $\phi(\mathbf{r})$. Similarly, solvent molecules are considered to be in a field of ω_S conjugates to the solvent density field $f_S(\mathbf{r})$. Hence, free energy of the DBC in selective solvents is given by:

$$\begin{aligned} NF / k_B T\rho_0 V = & -f_P \ln(Q_P / f_P V) - f_S \ln(\alpha_S Q_S / f_S V) \\ & + (1/V)\int d\mathbf{r}\Bigg[\sum_{i,j\in A,B,C,S;i\neq j} \chi_{ij} N\phi_i(\mathbf{r})\phi_j(\mathbf{r}) \\ & - \sum_{i=A,B,C,S} \omega_i(\mathbf{r})\phi_i(\mathbf{r}) - \xi(\mathbf{r})(1 - \sum_{i=A,B,C,S} \phi_i(\mathbf{r}))\Bigg] \end{aligned} \quad (1)$$

Where $\xi(\mathbf{r})$ is the potential field that ensure the incompressibility of the system, also known as a Lagrange multiplier and χ_{ij} is a Flory–Huggins interaction parameter

between different block species i and j. Q_P is the partition function of a single dendrimer chain subject to the mean field of DBC (ω_i) and independent of the contour length parameter of the chain, s. It can be written as $Q_P = \int \mathrm{d}\mathbf{r} q_i(\mathbf{r},s) q_i^+(\mathbf{r},s)$ in terms of $q_i(\mathbf{r},s)$ and $q_i^+(\mathbf{r},s)$. The $q_i(\mathbf{r},s)$ is distribution function, representing the probability of finding segment s at position $\mathbf{r}$. It satisfies a modified diffusion equation using a flexible Gaussian chain model:

$$\frac{\partial}{\partial s} q_i(\mathbf{r},s) = \frac{Na^2}{6} \nabla^2 q_i(\mathbf{r},s) - \omega_i(\mathbf{r}) q_i(\mathbf{r},s) \tag{2}$$

Because the two ends of each block chain are distinct, a second end-segment distribution function $q_i^+(\mathbf{r},s)$ is needed, that satisfies Eq. (2) only with the right-hand side multiplied by –1. Each block chain of the DBC is parameterized with variable s, which increases along the chain. The branching points O_1, O_2 and O_3 correspond to s = 0. Along each block chain, say block chain O_1A, s increases from 0 at the branching point O_1 to $f_{O1A}N$ at the other end A of the block chain O_1A. The other eight block chains O_2A, O_3A, O_1B_1, O_1C_1, O_2B_2, O_2C_2, O_3B_3, and O_3C_3 are parameterized similarly.

With these definitions, the initial conditions of the above diffusion equations are

$$q^+_{\mathrm{O}_i\mathrm{B}_i}(\mathbf{r}, f_{\mathrm{O}_i\mathrm{B}_i}N) = q^+_{\mathrm{O}_i\mathrm{C}_i}(\mathbf{r}, f_{\mathrm{O}_i\mathrm{C}_i}N) = 1.0 \quad (i \in [1,3]) \tag{3}$$

$$\begin{gathered} q_{\mathrm{O}_i\mathrm{A}}(\mathbf{r},0) = q^+_{\mathrm{O}_j\mathrm{A}}(\mathbf{r},0) \cdot q^+_{\mathrm{O}_k\mathrm{A}}(\mathbf{r},0) \\ (i,j,k \in [1,3];\ i \neq j, i \neq k, j \neq k) \end{gathered} \tag{4}$$

$$q_{\mathrm{O}_i\mathrm{B}_i}(\mathbf{r},0) = q^+_{\mathrm{O}_i\mathrm{A}}(\mathbf{r},0) \cdot q^+_{\mathrm{O}_i\mathrm{C}_i}(\mathbf{r},0) \quad (i \in [1,3]) \tag{5}$$

$$q_{\mathrm{O}_i\mathrm{C}_i}(\mathbf{r},0) = q^+_{\mathrm{O}_i\mathrm{A}}(\mathbf{r},0) \cdot q^+_{\mathrm{O}_i\mathrm{B}_i}(\mathbf{r},0) \quad (i \in [1,3]) \tag{6}$$

$$\begin{gathered} q_{\mathrm{O}_i\mathrm{A}}(\mathbf{r}, f_{\mathrm{O}_i\mathrm{A}}N) = q^+_{\mathrm{O}_j\mathrm{A}}(\mathbf{r}, f_{\mathrm{O}_j\mathrm{A}}N) \cdot q^+_{\mathrm{O}_k\mathrm{A}}(\mathbf{r}, f_{\mathrm{O}_k\mathrm{A}}N) \\ (i,j,k \in [1,3];\ i \neq j, i \neq k, j \neq k) \end{gathered} \tag{7}$$

$Q_S = \int \mathrm{d}\mathbf{r} \exp(\alpha_S \omega_S(\mathbf{r}))$ is the partition function of the solvent in the effective chemical potential field ω_S.

Minimizing the free energy of Eq. (1) with respect to ϕ_i and ω_i, $\delta F/\delta\phi = \delta F/\delta\omega$,

leads to the following self-consistent field equations that describe the morphology of phase separation:

$$\omega_i(\mathbf{r}) = \sum_{i,j\in A,B,C,S} \chi_{ij} N\phi_j(\mathbf{r}) + \xi(\mathbf{r}) \quad (i \neq j) \tag{8}$$

$$\sum_{i\in A,B,C,S} \phi_i(\mathbf{r}) = 1.0 \tag{9}$$

$$\phi_A(\mathbf{r}) = \frac{f_P V}{NQ_P} \sum_{i\in[1,3]} \int_0^{f_{\mathrm{O}_i\mathrm{A}}N} \mathrm{d}s q_{\mathrm{O}_i\mathrm{A}}(\mathbf{r},s) q^+_{\mathrm{O}_i\mathrm{A}}(\mathbf{r},s) \tag{10}$$

$$\phi_B(\mathbf{r}) = \frac{f_P V}{NQ_P} \sum_{i\in[1,3]} \int_0^{f_{\mathrm{O}_i\mathrm{B}_i}N} \mathrm{d}s q_{\mathrm{O}_i\mathrm{B}_i}(\mathbf{r},s) q^+_{\mathrm{O}_i\mathrm{B}_i}(\mathbf{r},s) \tag{11}$$

$$\phi_C(\mathbf{r}) = \frac{f_P V}{NQ_P} \sum_{i\in[1,3]} \int_0^{f_{\mathrm{O}_i\mathrm{C}_i}N} \mathrm{d}s q_{\mathrm{O}_i\mathrm{C}_i}(\mathbf{r},s) q^+_{\mathrm{O}_i\mathrm{C}_i}(\mathbf{r},s) \tag{12}$$

$$\phi_S(\mathbf{r}) = \frac{f_S V}{Q_S} \exp(-\alpha_S \omega_S(\mathbf{r})/N) \tag{13}$$

Eqs. (8)–(13) are a closed set of self-consistent equations, which are solved directly in real space by using a combinatorial screening algorithm proposed by Drolet and Fredrickson.[23] The algorithm consists of randomly generating an initial random distribution of concentration with fluctuation amplitude of 10^{-4} for f_P. The diffusion equations are then integrated to obtain $q_i(\mathbf{r},s)$ and $q_i^+(\mathbf{r},s)$ for for $0 < s < f_iN$, where f_i representing the volume fraction of each block chain. Then the right-hand sides of Eqs. (10)–(13) are evaluated to obtain new values for the volume fractions of block A, B and C, and solvent S.

Generally, the SCFT can be used to make the statistical analysis on the information of the primary structure (bond length, bond angle, etc.) of the polymer, and then to get the information of secondary structure (different block segment of polymer) and the tertiary structure, say, the different morphologies displayed in this work. Our current SCFT model does not contain the primary structure (such as H-bond) nor does it retain the angular spatial information needed to describe the aggregates of dendrimer. However, there is a few results reported by the other single chain theory that is quite different from the model used in this work, and the model used here is more easy to discuss the information of the secondary structure (block

segment), tertiary structure (morphologies displayed in this work) and even the textural structure.

To understand the relationship between morphological properties and chain architecture of dendrimer copolymers in a selective solvent, a systematic SCFT study is carried out in a cubic box with periodic boundary conditions along three directions. We assume that each block chain has an equal monomer statistical Kuhn length α, and then the grid sizes are chosen to be $d_x = d_y = d_z = \alpha$. We scale distances by Gaussian radius of gyration for the dendrimer which had been proposed by Zimm, $R_g = \alpha[(117/165)N/6]^{1/2}$,[30,31] and then the simulation box is chosen to sufficiently large $L = 40\alpha - 50\alpha$ and $L \geq 12R_g$ to avoid boundary effects on the morphological structure. Moreover, in the numerical calculations, the spatial average volume fraction of the DBC is set as $f_p = 0.1$, except for the phase diagram of f_P *vs* α_S, to ensure that the dendrimer system performs as a dilute solution. All the simulations are carried out until the phase patterns are stable and repeated by using different random numbers to guarantee the observed structures are not artifacts.

Our simulation subject is the asymmetric amphiphilic DBC in selective solvent, then three block segments in the first generation of the dendrimer are set as 6, 6, and 8, respectively, for block O_1A, O_2A, and O_3A in this work. Since the block C in DBC is hydrophilic, say the solvent is good for block C, consequently, the interaction parameters are set to be followings: $\chi_{AS} = \chi_{BS} = 1.5\chi_{ij}$ ($i,j \in$ A,B,C; $i \neq j$), $\chi_{CS} = 0$. Even though the internal structure of the solvent are not treated explicitly enough, the excluded volume effect is varied to consider the solvent size on the microphase separation of the amphiphilic DBC. We mainly consider the excluded volume effective parameter on the solvent size averages ranging from $\alpha_S = 0.5$ to 3. The relative magnitude between hydrophobic block B and hydrophilic block C in the second generation of the DBC are also considered.

III. Results and Discussion

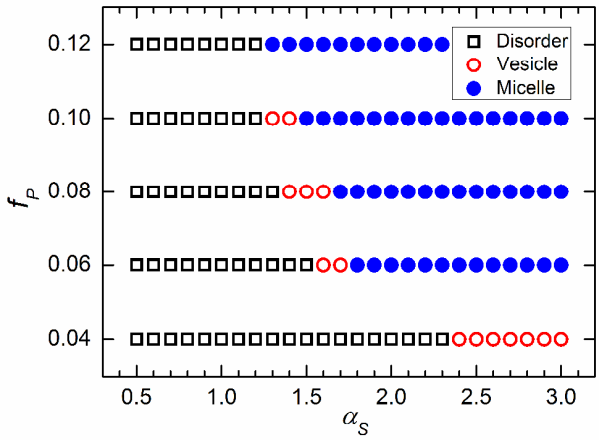

Fig. 2 Phase diagram of amphiphilic dendrimer solutions by continuously varying the dendrimer concentration f_P and the excluded volume effect parameter α_S with $N_B = N_C = 8$, $\chi_{ij} = 0.88$, $\chi_{AS} = \chi_{BS} = 1.5\chi_{ij}$, and $\chi_{CS} = 0$. Notes that different vesicular and micellar morphologies displayed in this phase diagram are collectively referred to as vesicle and micelle, respectively.

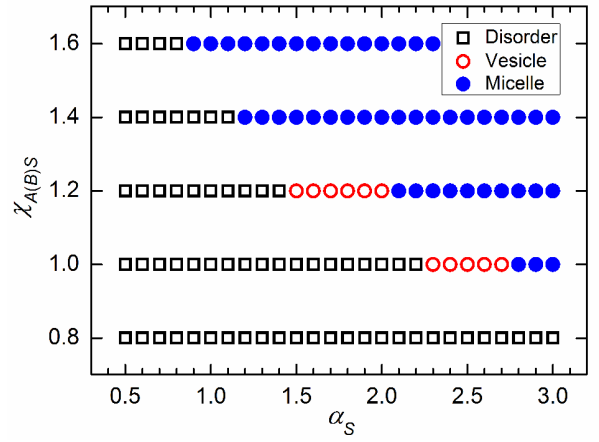

Fig. 3 Phase diagram of amphiphilic dendrimer solutions by continuously varying the interaction parameters of dendrimer/solvent $\chi_{A(B)S}$ ($\chi_{AS} = \chi_{BS}$) and the excluded volume effect parameter α_S with $N_B = N_C = 8$, $\chi_{ij} = 0.8$, and $\chi_{CS} = 0.0$. Notes that different vesicular and micellar morphologies displayed in this phase diagram are collectively referred to as vesicle and micelle, respectively.

To highlight the effect of molecular size of selective solvent, the amphiphilic dendrimer block copolymer (DBC) with equal arm of block B and block C ($N_B = N_C = 8$) in selective solvent with an exclude volume effect parameter α_S in a range from 0.5 to 3.0 has been investigated by 3D real-space SCFT (Fig. 2, 3).

It is consciously to choose a nearly symmetric $A_{20}B_{24}C_{24}$ dendrimer with the constant interaction parameters of $\chi_{ij} = 0.88$, $\chi_{AS} = \chi_{BS} = 1.5\chi_{ij}$, and $\chi_{CS} = 0$ (Fig. 2), and to discover the relationship between the excluded volume effect and the

dendrimer concentration f_P. Fig. 2 shows that there are two morphological transitions of disorder-to-order and order-to-order appear in the medium concentration of dendrimer (f_P = 0.06, 0.08, and 0.10). Unlike these, only one disorder-to-order transition can be observed in the boundary concentration, the ordered aggregate of vesicle for smaller one f_P = 0.04, while the micellar morphology takes the controlling position of the ordered segregate for the bigger one f_P = 0.12. Totally, the aggregate dendrimer concentration decreases with the stronger excluded volume effect. Fig. 2 illuminates well that the excluded volume effect increases and resulting in an order-to-order transition occurs, in which it finally achieves the morphological transition from vesicle to micelle. It is attributed to the natural quality of the solvent, in which the larger size of the solvent, the stronger excluded volume effect of it and the larger depletion it has. To further confirm these, the interactions of dendrimer/solvent $\chi_{A(B)S}$ ($\chi_{AS} = \chi_{BS}$) how to effect on morphological transition have been shown in Fig. 3. It shows that when the $\chi_{A(B)S}$ is equal to the interaction parameters χ_{ij}, $\chi_{A(B)S} = \chi_{ij}$ = 0.8, the denerimer solution system takes a disordered morphology in range of the excluded volume effect parameter from 0.5 to 3.0. It due to the microphase separation of amphiphilic dendrimer taking place in the conditions of $\chi_{A(B)S} > \chi_{ij}$ and $\chi_{CS} << \chi_{ij}$, which agrees well with the fact that the block A and B are hydrophobic, while the block C is hydrophilic in the amphiphilic dendrimer. Similarly, there are two morphological transitions of disorder-to-vesicle and vesicle-to-micelle can be observed with the smaller interaction parameters of dendrimer/solvent ($\chi_{A(B)S}$ = 1.0, 1.2), and then only one disorder-to-micelle can be observed with increasing its value to the bigger ones $\chi_{A(B)S}$ =1.4 and 1.6. The dendrimer solution within the stronger segregation regime $\chi_{A(B)S}$ results in the appearance of the ordered aggregates with the weaker excluded volume effect. It means that it is easier to achieve the morphological transition from vesicle to micelle with increasing the interaction parameters of dendrimer/solvent. To have a better understanding of the phenomenon of the morphological transition from vesicle to micelle, the following parts aim at taking detailed the interaction of dendrimer/solvent and the relative length of the second generation of the dendrimer with a constant dendrimer concentration f_P = 0.1

into consideration. For the former, it appears in the state of the segregation degree of different block segments (χ_{ij}), i.e., $\chi_{A(B)S}$ = 1.5 χ_{ij} and χ_{CS} =0, such as the middle row of dendrimer/solvent interaction $\chi_{A(B)S}$ = χ_{ij} 1.5 effects on the microphase separation of dendrimer solution shown in Fig. 3.

A. Segregation degree dependence

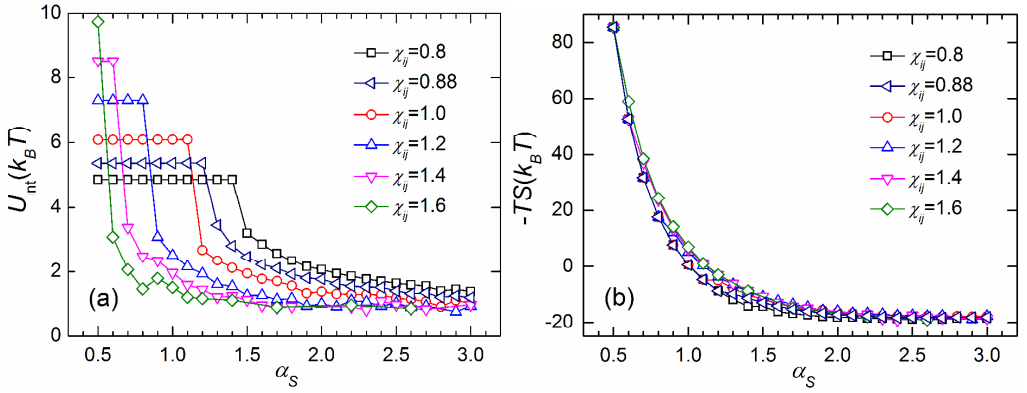

Fig. 4 Free energy variation of amphiphilic dendrimer solution as a function of excluded volume effect parameter α_S with N_B = N_C = 8 according to different interaction parameter from χ_{ij} = 0.8 to χ_{ij} = 1.6, respectively, and χ_{AS} = χ_{BS} = 1.5χ_{ij}, χ_{CS} = 0.

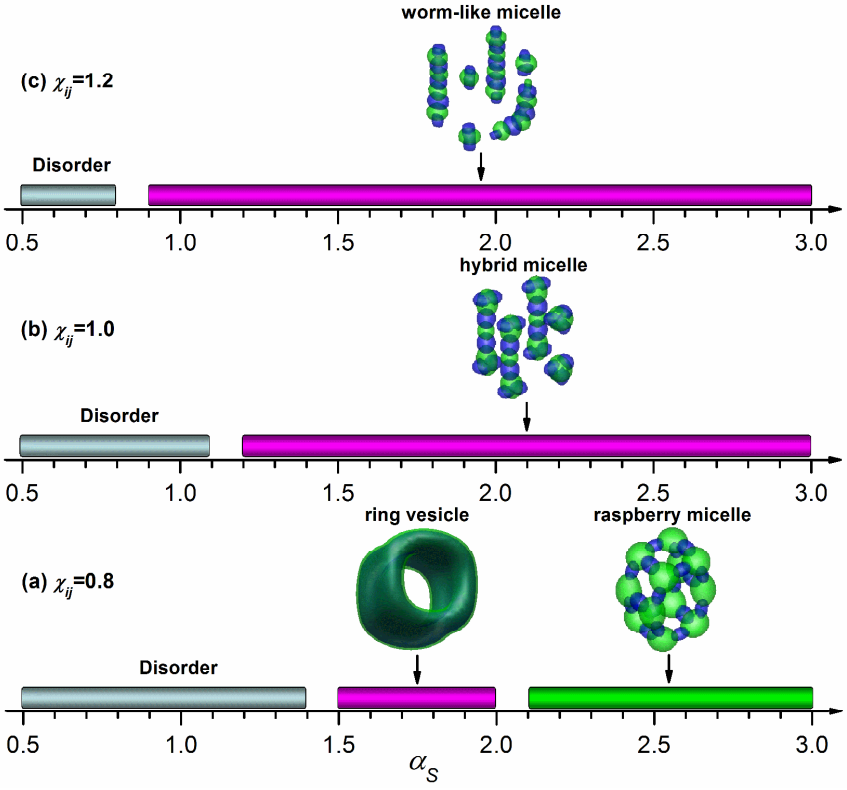

Fig. 5 Morphological transition of amphiphilic dendrimer solution induced by the excluded volume effect parameter α_S with $N_B = N_C = 8$ and different interaction parameters (a) $\chi_{ij} = 0.8$, (b) $\chi_{ij} = 1.0$, (c) $\chi_{ij} = 1.2$, and $\chi_{AS} = \chi_{BS} = 1.5\chi_{ij}$, $\chi_{CS} = 0$. The morphology shown in each appointed range of α_S is the characteristic snapshot. The Blue and green in the isosurface graphs represents hydrophobic block A and B in the dendrimer, while hydrophilic block C and solvent S are omitted for clarity.

The ability of highly asymmetric amphiphilie to assemble into a variety of morphologies, including sphere, rod, tubules, hexagonally packed hollow hoops, large compound micelles (LCMs) and large compound vesicles (LCVs), which can be manipulated by the relative block lengths and environmental parameters, such as solvent composition, the presence of additives and temperature.[32] These aggregates are governed by a balance of three contributions of free energy including core-chain stretching, interfacial energy and the intercoronal chain interactions.[33]

While in SCFT, the statistical analysis on the information of the primary structure results in a free energy, consequently, the free energy of the dendrimer solution system has been evaluated by $F = U_{\text{int}} - TS$ and can be divided into two parts: the interfacial free energy (U_{int}) and the entropic free energy ($-TS$). The interfacial energy item is expressed as,

$$U_{\text{int}} = (1/V)\int \mathrm{d}\mathbf{r} \sum_{i,j\in A,B,C,S;i\neq j} \chi_{ij} N \phi_i(\mathbf{r})\phi_j(\mathbf{r}) \qquad (14)$$

and the entropic contribution of the dendrimer solution system is written as,

$$-TS = -f_P \ln(Q_P / f_P V) - f_S \ln(Q_S / f_S V) + (1/V)\int \mathrm{d}\mathbf{r} \sum_{i\in A,B,C,S} \omega_i(\mathbf{r})\phi_i(\mathbf{r}) . \qquad (15)$$

The energy distribution of the dendrimer solution that induced by the solvent with different excluded volume effect shown as Fig. 4. Before the disorder-to-order transition, the interfacial free energy U_{int} keeps constant (Fig. 4a) and the entropic free energy $-TS$ (Fig. 4b) is dominant in the free energy F. As a result, it totally can be found that the free energy decrease with increasing the excluded volume effect (α_S) generally for different interaction parameters of block species from $\chi_{ij} = 0.8$ to $\chi_{ij} = 1.6$. However, a distinct phenomenon attracts our attention that the ordered aggregates can be observed firstly at the beginning of the sharp fall of the interfacial free energy, and the first value of α_S that begins to appear the ordered aggregate decreases with increasing the interaction parameter χ_{ij}. Meanwhile, the disordered phases are

ubiquitous when the α_S is very weak and the depletion effect is usually strong with increasing the α_S, consequently, leads to the dendrimer copolymer taking a clear phase separation. In other words, the ordered region of segregate becomes broader according to enlarging the repulsion between the different block species of the dendrimer shown as Fig. 5. However, the energy ($F = U_{\text{int}} - TS$) change is not obvious for the order-to-order transition of aggregates in the case of equal arms of second generation in the dendrimer, which corroborated by Li *et al*[16] that the morphological shift from vesicle to micelle had been obtained with increasing the molecular size of solvent.

For the ordered segregates, they are always observed in the stronger excluded volume effect within a strong segregation regime, and there is a morphological shift from ring vesicle to raspberry micelle at the less interaction parameter of $\chi_{ij} = 0.8$ (Fig. 5a). For latter, there are three B beads dispersed on a large C core appear corresponding to raspberry-like micelles. Raspberry morphologies have been observed firstly in linear terpolymer bulk[34] and its aqueous both by experiments and simulations[35,36], and later in the star terpolymer aqueous by theoretic simulations.[26] Dormidontova and Khohklov had predicted the similar structure for the linear terpolymers in strong and even super strong segregation limit.[37] Our simulation results show that raspberry micelle occurs at the strong regime of excluded volume effect and the strong segregation of block species. It is consistent with the experimental results and predictions that raspberry micelles only appear in the strong segregation regime of copolymers. In the strong segregation regime of block copolymers ($\chi_{ij} \geq 0.5$),[31] the first generation of the dendrimer by forming beads is dispersed around the block B forming core, which can decrease the interfacial energy of blocks. Moreover, another ordered segregates of hybrid micelle mixing worm-like micelle and raspberry micelle within a more strong regime of segregation, such as $\chi_{ij} = 1.0$ (Fig. 5b), is observed in the stronger regime of α_S, in which the molecular size of solvent is still bigger ($\alpha_S \geq 1.2$) than the normal size of solvent molecule $\alpha_S = 1.0$. When the interaction parameter further increasing to $\chi_{ij} = 1.2$ (Fig. 5c), the ordered morphologies of long segmented worm-like micelle along with short segmented worm-like micelle, say hamburger, can be found with a less solvent size of weak excluded volume effect $\alpha_S \geq 0.9$. This

contributes to the entropic free energy (-*TS*) can offset the repletion effect of the selective solvent for the dendrimer very well with increasing the segregation degree χ_{ij}. Eisenberg *et al*.[38] had pioneered the field of micellar morphology control with the so-called "crew-out" micelles. In particular, it was demonstrated lately that amphiphilic copolymers containing more than one hydrophobic block arm which are incompatible to each other can self-assemble in solvent into subdivided multicompartment micelles, such as worm-like micelle and sphere micelle in this work.

B. Hydrophobic block length dependence

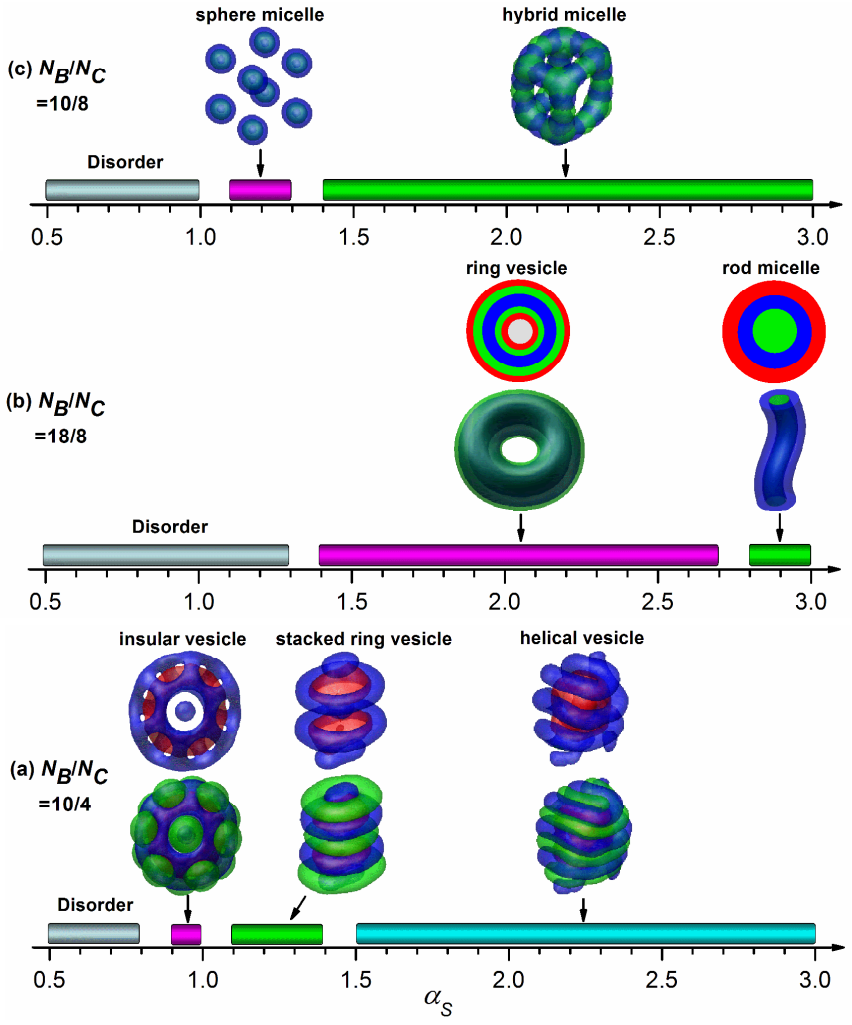

Fig. 6 Morphological transition of amphiphilic dendrimer solution induced by the excluded volume effect parameter α_S at χ_{ij} = 60/62, χ_{AS} = χ_{BS} = 1.5χ_{ij}, χ_{CS} = 0, (a) N_B =10, N_C =4; (b) N_B =18, N_C =8; (c)

N_B =10, N_C =8. The morphology shown in each appointed range of α_S is the characteristic snapshot. The blue, green and red represents block species of A, B, and C in the dendrimer, while solvent S and block C (in case of b, c) are omitted for clarity.

Since the segregation degree has been found for its compensating action for the excluded volume effect in controlling the morphological shift from vesicle to micelle on the second generation of dendrimer with the equal arms shown as Fig. 4 and Fig. 5. In this part, we attach importance to the asymmetry of the hydrophobic block B and hydrophilic block C on the microphase separation of the dendrimer solution at $N_B > N_C$ within a strong segregation degree of χ_{ij} = 60/62[31] (Fig. 6). The disordered morphologies always appear in the regime of lower excluded volume effect parameter, $\alpha_S \leq 0.8$ for the case of N_B =10, N_C =4 (Fig. 6a); $\alpha_S \leq 1.3$ for the case of N_B =18, N_C =8 (Fig. 6b); while $\alpha_S \leq 1.0$ for the case of N_B =10, N_C = 4 (Fig. 6c). Fig. 6a shows that the basic building unit of the ordered morphology of vesicle is a bilayer comprising inner and outer cavity, where hydrophilic block C lies in the inner and outer side surfaces of the vesicle in contact with the solvent directly. The top row of Fig. 6a illuminates that the density of the hydrophilic block C on the internal surface of the vesicle is always higher than that on the outside. It is a common phenomenon that due to the curvature of the vesicle the outside cavity has more space for polymer chain stretching, while on the inside, chains should be packed up, and thus leads to higher density distribution near the inner wall than the outside.[39] Moreover, an order-to-order transition of the total vesicle is observed and undergoes a morphological transition from insular structure to stacked ring, and finally to helical structure at the bigger relative magnitude of N_B/N_C=10/4 (Fig. 6a). The transition of undistorted vesicle to distorted vesicle, which is attributed to excluded volume effect of solvent molecule become stronger and stronger, and then the solvent with larger size has the stronger depletion or excluded volume interaction[14] on the dendrimer in the appointed space. The essence is the dendrimer with low generation in this work is flexible, thus, both the inner block A and outer block B of the dendrimer can come into contact with the outside of the vesicle.[40] This interaction is expected to produce distortions of the dendrimer molecule, and the degree of distortion depending on the nature of the solvent, i.e. molecular size. Another reasonable explanation is the confinement

increasing with the diameter of solvent and the depletion is stronger for dendrimer, leads to the concentration among these bigger solvent is higher than the critical micelle concentration (CMC) of the dendrimer, the helical vesicle morphology occurs. The depletion effect is strong in dilute solution and will largely affect the amphiphilic dendrimer in solution for the ordered morphologies appear frequently in the strong regime of excluded volume effect in this work.

Then decreasing continually the ratio of N_B/N_C from 10:4 (Fig. 6a) to 18:8 (Fig. 6b), another morphological transition from ring vesicle to rod micelle has been observed at the similar stronger regime of α_S. The intersecting surface of morphologies in the top row of Fig. 6b show the schematic distribution of the different block species and the morphologies take an obvious shift from vesicle to micelle, which can clearly present the depletion from the excluded volume effect of the solvent on the self-assembly of the dendrimer. Except for the depletion effect, the molecular structure is also well worth considering that the appearance of rod micelle is because of the topological characteristics of dendrimer copolymer in which the immiscible blocks must converge at four junction points, the concentric structure found in this dendrimer solution is suppressed and micellar cylinder occurs. The peptide amphiphilie (PA, one of typical dendrimer) assemblies often results in high aspect ratio rod micelles which makes the spherical PA nanoparticles difficult to access.[41,42] Meanwhile, even though the vesicles appear both in Fig. 6a and Fig. 6b, short hydrophilic blocks (Fig. 6a) preferentially segregate to the inner surface of the vesicle while long hydrophilic blocks (Fig. 6b) tend to segregate to the outside of the vesicle.[39] Such a length segregation mechanism in the amphiphilic copolymers with different lengths had been confirmed from Eisenberg's experimental observations.[43]

Furthermore, when the ratio of N_B/N_C decrease to 10/8 (Fig. 6c), the ordered morphology take a direct shift from the vesicle (Fig. 6a, b) to the micellar structure (Fig. 6c), such as the sphere micelle and a hybrid structure that mixing worm-like micelle and raspberry-like micelle (Fig. 6c). In other words, the vesicular morphologies can easily be observed in dendrimer solution with increasing the ratio of N_B/N_C from 10/8 (Fig. 6c) to 18/8 (Fig. 6b) and then to 10/4 (Fig. 6a), which agrees

well with the experimental results reported by Zhang *et al.*[12] whom have pointed out that increases continuously hydrophobic alkyl chain length, where the cohesion among hydrophobic chain weaken the hydrophobic interactions, further increase the enthalpy and then leads to the appearance of vesicular structures.

C. hydrophilic block length dependence

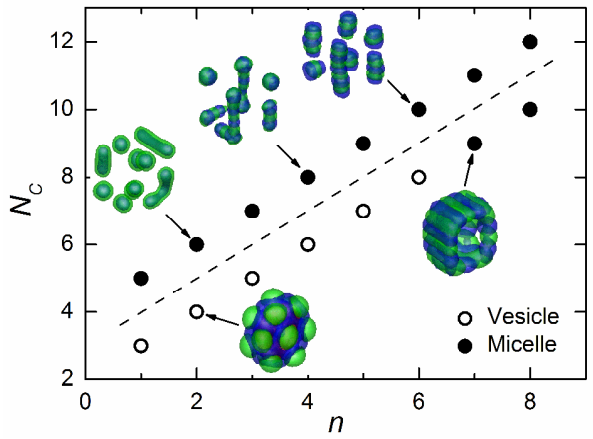

Fig. 7 Phase diagram of amphiphilic dendrimer solutions at $\alpha_S = 1.2$, $\chi_{ij} = 1.2$, $\chi_{AS} = \chi_{BS} = 1.5\chi_{ij}$, $\chi_{CS} = 0$. Above and below the visual guidance are according to the two different second generations of dendrimer $B_{2+n}C_{4+n}$ and $B_{8+n}C_{2+n}$, respectively.

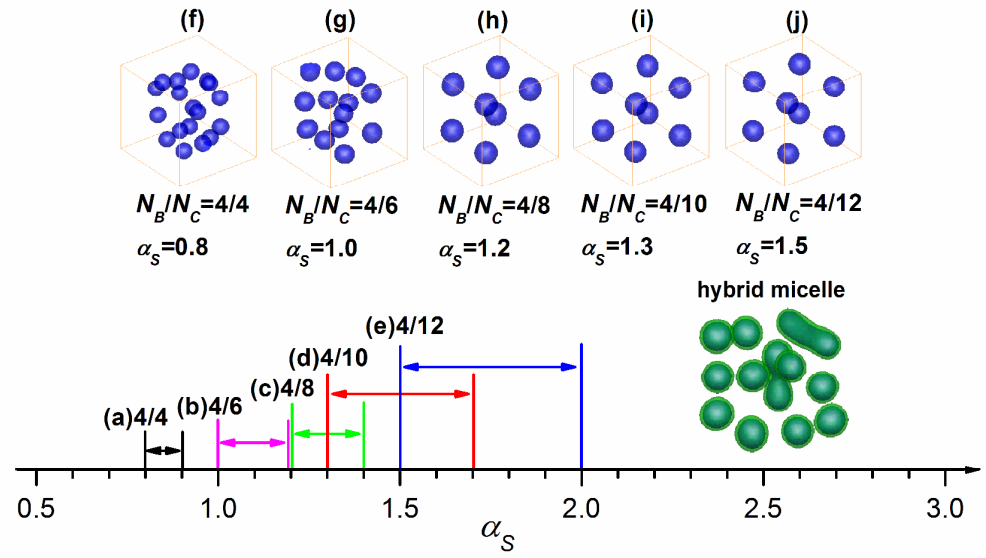

Fig. 8 Morphological transition of amphiphilic dendrimer solution induced by the excluded volume effect parameter α_S according to the different second generations of dendrimers of (a) N_B =4, N_C =4; (b) N_B =4, N_C =6; (c) N_B =4, N_C =8; (d) N_B =4, N_C =10; (e) N_B =4, N_C =12 with a constant interaction parameter $\chi_{ij} = 1.2$ and $\chi_{AS} = \chi_{BS} = 1.5\chi_{ij}$, $\chi_{CS} = 0$. Each horizontal bar in different colors represents the

regime of sphere micelle of different dendrimer, on the left of each horizontal bar is the disorder region, while the right represents the ordered regime of hybrid micelle that is mixture of sphere and rod displays in here is the characteristic snapshot when the α_S > 1.0, 1.3, 1.5, 1.8, and 2.1 from (a) to (e), respectively. The top row (from (f) to (j)) of this figure is the sphere micelle that firstly appears on the appointed excluded volume effect parameter that shown below the morphologies. For the hybrid micelle, blue and green in the isosurface morphologies represents hydrophobic block A and B in the dendrimer, while hydrophilic block C and solvent S are omitted for clarity; for the sphere micelle on the top row, block B, block C and solvent S are also omitted for clarity.

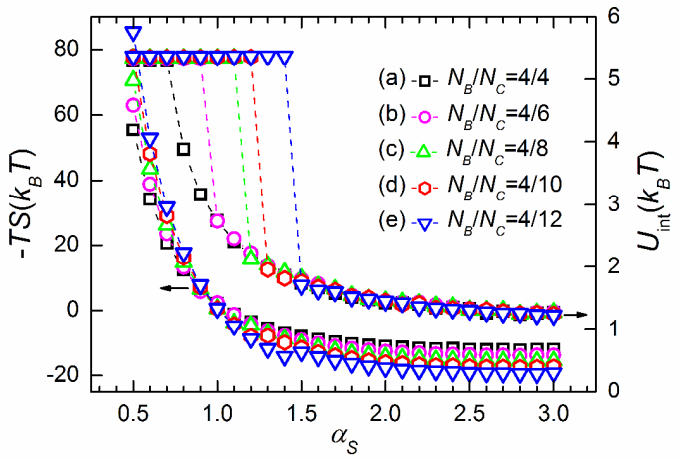

Fig. 9 Energy contribution of amphiphilic dendrimer solution as a function of excluded volume effect parameter α_S according to different dendrimers of (a) N_B =4, N_C =4; (b) N_B =4, N_C =6; (c) N_B =4, N_C =8; (d) N_B =4, N_C =10; (e) N_B =4, N_C =12 and the interaction parameter keeps unchanged χ_{ij} = 1.2 with χ_{AS} = χ_{BS} = 1.5χ_{ij}, χ_{CS} = 0.

In contrast to solvophobic forces (Fig. 6), here we intend to take an insight of the opposing effect in this part, say, the relative magnitude of block B and block C in the dendrimer copolymer is $N_C > N_B$, while the excluded volume effect parameter and interaction parameters remain unchanged $\alpha_S = \chi_{ij} = 1.2$ (Fig. 7). A phase diagram (Fig. 7) is given out as the space length of the second generation of dendrimer increases with an arithmetic sequence, which has characteristics of active chain growth on the chemical synthesis of dendrimer.[44,45] In Fig. 7, all of the vesicular and micellar morphologies are uniformly called vesicle and micelle without discussing the subtle difference between themselves, respectively. The dendrimer solution display an order-to-order transition from vesicle to micelle for the second generation of the dendrimer is $B_{8+n}C_{2+n}$ that is similar to Fig. 6. On the contrary, when the hydrophilic effect of block C is highlighted and enlarging its length, the micellar structure will be dominant in $B_{2+n}C_{4+n}$. It notes that the relative magnitude in chain length between the

hydrophilic block C and the hydrophobic block B can effect very much on the assembly of dendrimer solution. Even though $N_B > N_C$, the morphology of dendrimer solution has a shift from vesicle to micelle when the N_C is close to N_B (below the visual guidance in Fig. 7), and then the morphology takes an overwhelming micellar structure when the relative magnitude of the second generation of dendrimer turns to $N_C > N_B$ (above the visual guidance in Fig. 7). Since the structural shift tendency from vesicle to micelle has been evaluated according to the relative magnitude between the hydrophobic block segments N_B and the hydrophilic block segments N_C. So we focuses on the relative magnitude of N_C/N_B keeps increasing from 4/4 to 12/4 (Fig. 8, 9), with a relatively long block C and increasing the length of hydrophilic block C, the micellar morphology are observed consistently and changing from sphere micelle to hybrid micelle with a mixture of sphere and rod in the ordered morphological regime of the excluded volume effect shown as Fig. 8 a–e.

When the block C length increases, meanwhile the repulsive interactions between the second generation increases, consequently the surface area per second generation chain decreases. Therefore, more chain can aggregate, which leads to the larger sphere appears within the appointed space in a disperse manner. In this work, the number of spheres in the spherical morphologies per one unit of space volume is defined as $N_0 = N_{sp}/(R_g)^3$, and then its reciprocal type value is defined as the radii of sphere (R_d) in the spherical morphologies,

$$R_{sp} = R_g \left(\frac{3}{4\pi N_{sp}} \right)^{1/3} \tag{16}$$

To calculate the radius of gyration of the dendrimers (R_g), the mass of each sphere is assumed to be uniformly distributed in the sphere. Fig. 8 f–j show that the number of the spheres in the spherical morphology (N_{sp}) is 19, 13, 8, 8, and 8, respectively, from Fig. 8a to Fig. 8e, while the R_g increases according to Zimm[30,31] from 2.28α to 2.43α to 2.57α to 2.71α, and finally to 2.84α, respectively, from Fig. 8a to Fig. 8e. The Gaussian radius of gyration for the dendrimer $R_g = \alpha[(117/165)N/6]^{1/2}$ proposed by Zimm that used in this work which is the same as the scaling law

$R_g \sim \alpha(gs)^{1/2}$ reported by Boris *et al.*[29] whom considered a dendrimer of generation g with flexible spacer, where each spacer consists of s monomers of size α, and the Gaussian size of this dendrimer R_g is of the order of size of a linear strand of gs (N used in this work) monomers. Their theoretical results shown that this scaling law specially applied to the low generation of the dendrimer, i.e, $g \leq 5$, consequently, g = 2 in this work is a good proof of this scaling law. It is also consistent with the Flory-theory for dendrimers that incorporates three body interactions, which was proposed by Sheng[46] who emphasized the importance of the three-body interactions on the densely packed nature of the dendrimers and further promoted by Prakash *et al.*[2] in their Brownian dynamics simulations. In their theory, the radius of gyration R_g obeys a scaling law $R_g \sim N^{1/5}(g+1)^{2/5}b^{2/5}$ according to the parameters characterizing dendrimer architecture, where N is the total number of monomers in the dendrimer, g is the number of generation, and b is the number of monomers in the chain called spacers. The increasing of N and b is equal to the increasing of the number of monomer in block segment C (N_C) in this work even though the numbers of generation (g) keeps constants, and then as a result of $N_C \uparrow$, the radius of gyration gets $R_g \uparrow$. The experimentally measurable quantity that characterizes the dendrimer size is its radius of gyration R_g. Another measure is the corona radius R_c that introduced by Daoud *et al.*[47] in their framework of the standard blob model of a dendrimer and further developed in the work of Likos[48], defining as the distance from the center of the dendrimers in which all monomers are 'inside'. In this model, the inner of the dendrimer is regarded as a succession of concentric shells of blobs, each blob in the shell having a certain size. The spherical blobs are closely packed and within each one every chain behaves as if it were free, i.e., the effects of the neighboring chains are not present. Consequently, the corona radius R_c scales by purely geometrical arguments as

$$R_c \sim \left[Nf + \frac{1}{10}\frac{f^{3/2}}{\bar{v}^2} + \frac{1}{6}f^{3/2} \right]^{3/5} \bar{v}^{1/5} f^{-2/5} \alpha , \qquad (17)$$

depending on the length of the chain N, the strength of the excluded volume interactions $\overline{v}$ (interaction parameters of different block species used in this work) and the functionality f (the derdrimer with trifunctionality here). Then one can distinguish dendrimer in the selective solvent that most of the dendrimer is in the swollen region, so that the core and the unswollen part of the dendrimer can be ignored, resulting in a reduced scaling law as follows:

$$R_c \sim N^{3/5}\overline{v}^{1/5} f^{1/5}\alpha \quad (N >> f^{1/2}\overline{v}^{-2}) \tag{18}$$

As can be seen from Eq (18) above, the spatial extension of dendrimers is larger than that of an isolated chain with the same length of the chain, due to stretching of the chains caused by the dendrimer architecture.[48] Based on these, these parameters keep constants except for the length of the dendrimer chain. Consequently, the corona radius, i.e., the radius (R_{sp}) of each sphere in spherical morphology, is increasing with the length of the hydrophilic block C in this work $N_C \uparrow \rightarrow R_c \uparrow \rightarrow R_{sp} \uparrow$.

It is agree well with the results from the SCFT used in this work, which the radii (R_{sp}) of the sphere in each spherical morphology increasing from 0.52α to 0.64α to 0.80α to 0.84α, and then to the biggest value of 0.88α, respectively, from Fig. 8a to Fig. 8e. These data of radii of spheres have been confirmed by the energy analysis of SCFT shown in Fig. 9. The right of Fig. 9 shows that the disordered region with weak excluded volume effect is controlled by interfacial free energy U_{int} and with a same constant energy value U_{int} = 5.4 k_BT according to the same interaction parameter χ_{ij} = 1.2. Consequently, the first value of excluded volume effect that appears the spherical morphology is exactly confirmed by Fig. 8 f–j, which fully illuminates the accuracy of SCFT on the prediction of morphology. The increasing in sphere radius leads to stretching of the hydrophobic block A and B, which implies that the larger the hydrophobic core, the higher the average degree of the hydrophobic chain stretching will be. This stretching is accompanied with a decrease of entropy shown as the entropic free energy (–TS) in the left of Fig. 9. After that the

aggregates become very larger, the entropic penalty of the hydrophobic block stretching renders simple spherical structures unfavorable with a less energy. In short, the less entropy the dendrimer solution is, the bigger radii of spherical (ordered) morphology is, that induced by lower excluded volume effect. Then the entropy of dendrimer solution continually deceases according to α_S with increasing the hydrophilic block segment (on the left of Fig. 9), consequently, a reduction in the degree of hydrophobic chain stretching is attributed to the appearance of the hybrid micelle that is a mixture of sphere and rod with decreasing the diameter of spherical morphologies. This simple structural transition of sphere to rod is due to the decrease in the hydrophobic block repulsion.

IV. Conclusions

In this work, the selective solvent with different molecular size effect on structural and phase transition aspects of amphiphilic dendrimer solution is investigated by regulating the excluded volume effect parameter (α_S) with an implementation of 3D real space SCFT. The selective solvent with stronger α_S makes the local concentration of the dendrimer higher than critical aggregate concentration (CAC), so the dendrimer will easily aggregate into an ordered morphology. To achieve the objective of taking an insight into the relative magnitude between the hydrophobic block B and hydrophilic block C on the segregation of dendrimer solution, the ratio of N_B/N_C has a significant influence on the assemblies. For $N_B = N_C = 8$, an order-to-order transition from vesicle to micelle is observed in a broader regime of stronger α_S with increasing the interaction parameter of block species, meanwhile, it points out that the disordered region of segregates is controlled by the interfacial free energy U_{int}. To proof deeply the role of the excluded volume effect on the microphase separation, the solvophobic forces are emphasized intendedly by regulating the ratio of N_B/N_C to $N_B > N_C$. The value of N_B/N_C is bigger; the vesicular morphology is more easily to be observed. The appearance of the distorted vesicle mainly due to the depletion effect of selective solvent for the dendrimer, and the CMC

of amphiphilic dendrimer will decrease. Moreover, N_C further increasing to $N_C > N_B$, the typical sphere micelle has been found with the ratio of N_C/N_B increasing from 4/4 to 12/4. Then it takes a morphological transition from spherical micelle to hybrid micelle that is a mixture of sphere and rod. The existence of sphere micelle and the order-to-order transition of morphology are mainly attributed to the decrease in the hydrophobic block repulsion that determined by entropic free energy ($-TS$). These results are useful in understanding the structural shift of the amphiphilie solution in the field of soft matter.

Acknowledgements

B. L gratefully acknowledges the financial support from the National Natural Science Foundation of China (Grant No. 21204012) and Guangdong Natural Science Foundation (Grant No. S2012040007981). We also thank for the technical support from National Supercomputing Center in Guangzhou, China.

References

[1]M. V. Walter and M. Malkoch, *Chem. Soc. Rev.*, 2012, **41**, 4593.
[2]J. T. Bosko and J. R. Prakash, *Macromolecules*, 2011, **44**, 660.
[3]A. Caminade, A. Ouali, M. Keller and J. Majoral, *Chem. Soc. Rev.*, 2012, **41**, 4113.
[4]J. Satija, V. V. R. Sai and S. Mukherji, *J. Mater. Chem.*, 2011, **21**, 14367.
[5]W. T. Tian and Y. Q. Ma, *Chem. Soc. Rev.*, 2013, **42**, 705
[6]M. Ainalem and T. Nylander, *Soft Matter*, 2011, **7**, 4577.
[7]K. L.Wooley, C. A. King, K. Tasaki and J. J. Schaefer, *J. Am. Chem. Soc.*, 1997, **119**, 53.
[8]A. Asteriadi, R. Sigel, D. Vlassopoulos, G. Meier, J. R. Dorgan and D. M. Knauss, *Macromolecules*, 2004, **37**, 1016.
[9]W. T. Tian and Y. Q. Ma, *Soft Matter*, 2011, **7**, 500.
[10]J. J. Freire, E. Rodriguez and A. M. Rubio, *J. Chem. Phys.* 2005,**123**, 154901.
[11]J. J. Freire, *Soft Matter*, 2008, **4**, 2139.
[12]P. Zhang, X. H. Xu, M. H. Zhang, J. B. Wang, G. Y. Bai and H. K. Yan, *Langmuir*, 2015, **31**, 7917.

[13]K. R. Raghupathi, J. Guo, O. Munkhbat, P. Rangadurai and S. Thayumanavan, *Acc. Chem. Res.*, 2014, **47**, 2200.

[14]R. Wang, Z. B. Jiang and G. Xue, *Polymer*, 2011, **52**, 2361.

[15]R. J. Spontak, R. Shankar, M. K. Bowman, A. S. Krishnan, M. W. Hamersky and J. Samseth, *Nano Letters*, 2006, **6**, 2115.

[16]W. Li and W. Jiang, *Macromol. Theo. Simul.*, 2009, **18**, 434.

[17] S. V. Lyulin, L. J. Evers, P. van der Schoot, A. A. Darinskii, A. V. Lyulin and M. A. J. Michels, *Macromolecules*, 2004, **37**, 3049.

[18]S. V. Lyulin, A. V. Lyulin and A. A. Darinskii, *Polym. Sci. Ser. A*, 2004, **46**, 189.

[19]W. D. Tian and Y. Q. Ma, *Soft Matter*, 2010, **6**, 1308.

[20]S. Huissmann, C. N. Likos and R. Blaak, Macromolecules, 2012, **45**, 2562.

[21]P. Welch and M. Muthukumar, *Macromolecules*, 1998, **31**, 5892.

[22]J. S. Klos and J. U. Sommer, *Macromolecules*, 2010, **43**, 4418.

[23]S. L. Mayo, B. D. Olafson and W. A. Goddard, *J. Phys. Chem.*, 1990, **94**, 8897.

[24]P. Carbone and F. Müller-Plathe, *Soft Matter*, 2009, **5**, 2638.

[25] F. Drolet and G. H. Fredrickson, *Phys. Rev. Lett.* 1999, **83**, 4317.

[26]J. W. Ma, X. Li, P. Tang and Y. L. Yang, *J. Phys. Chem. B*, 2007, **111**, 1552.

[27]Y. Jiang, T. Chen, F. W. Ye, H. J. Liang and A. C. Shi, *Macromolecules*, 2005, **38**, 6710.

[28]P. G. de Gennes and H. Hervert, *J. Phys., Lett.*, 1983, **44**, 351.

[29]D. Boris and M. Rubinstein, *Macromolecules*, 1996, **29**, 7251.

[30]B. H. Zimm and W. H. Stockmayer, *J. Chem. Phys.*, 1949, **17**, 1301.

[31]B. Lin, H. D. Zhang, P. Tang, F. Qiu and Y. L. Yang, *Soft Matter*, 2011, **7**, 10076.

[32]J. A. Opsteen, J. J. L. M. Cornelissen and J. C. M. van Hest, *Pure Appl. Chem.*, 2004, **76**, 1309.

[33]A. Halperin, M. Tirrell and T. P. Lodge, Adv. Polym. Sci., 1992, **100**, 31.

[34]S. Ritzenthaler, F. Court, E. Girard-Reydet, L. Leibler and J. P. Pascault, *Macromolecules*, 2003, **36**, 118.

[35]A. Laschewsky, *Curr. Opin. Colloid Interface Sci.*, 2003, **8**, 274.

[36]J. Xia and C. L. Zhong, *Macromol. Rapid Commun*. 2006, **27**, 1110.

[37]E. E. Dormidontova and A. R. Khokhlov, *Macromolecules*, 1997, **30**, 1980.

[38]L. B. Luo and A. Eisenberg, *J. Am. Chem. Soc.*, 2001, **123**, 1012.

[39]X. Li, P. Tang, F. Qiu, H. D. Zhang and Y. L. Yang, *J. Phys. Chem. B*, 2006, **110**, 2024.

[40]Y. S. Seo, K. S. Kim, K. Shin, H. White, M. Rafailovich and J. Sokolov,

Langmuir, 2002, **18**, 5927.

[41]B. F. Lin, R. S. Marullo, M. J. Robb, D. V. Krogstad, P. Antoni, C. J. Hawker, L. M. Campos and M. V. Tirrell, *Nano Lett*. 2011, **11**, 3946.

[42]M. J. Webber, J. A. Kessler and S. I. Stupp, *J. Intern. Med*. 2010, **267**, 71.

[43]O. Terreau, L. B. Luo and A. Eisenberg, *Langmuir*, 2003, **19**, 5601.

[44]H. S. Yoo, T. Watanabe, Y. Matsunaga and A. Horao, *Macromolecules*, 2012, **45**, 100.

[45]H. F. Zhang, J. P. He, C. Zhang, Z. H. Ju, J. Li and Y. L. Yang, *Macromolecules*, 2012, **45**, 828.

[46]Y. J. Sheng, S. Jing and H. K. Tsao, *Macromolecules*, 2002, **35**, 7865.

[47]M. Daoud and J. P. Cotton, *J. Phys*. (Paris), 1982, **43**, 531.

[48]C. N. Likos, *Soft Matter*, 2006, **2**, 478.